Windmill-Type Molecules for Efficient Deep-Blue Organic Light-Emitting Diodes via Hybridized Local and Charge-Transfer Excited-State

Huihui Li,[a,‡] Min Wang,[b,‡], Ziting Zhong [a] Hua Lu,[a,*] Zujin Zhao*,[b] and Xin Jiang Feng*,[a]

I. Supplementary Figures and Tables.

I. Supplementary Figures and Tables.

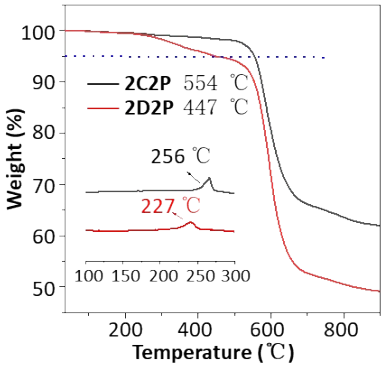

Fig. S1 Thermogravic analysis (TGA) traces for **2C2P** and **2D2P**. Inset: differential scanning calorimetry (DSC) traces.

Table S1 Photophysical properties of 2**C2P** and **2D2P** in solvents.

	Solvent	λ_{abs} [a] (nm)	λ_{em} [a] (nm)	$\Delta\nu_{em\text{-}abs}$ [b] (cm^{-1})	Φ_F [c]	τ_F [d] (ns)	K_r [e] (10^8 s^{-1})	K_{nr} [e] (10^8 s^{-1})
2C2P	Hexane	380	415	2219	0.66	1.45	4.55	2.34
	Toluene	365	418	3474	0.84	1.27	6.61	1.26
	DCM	363	429	4238	0.91	1.45	6.28	0.62
	THF	365	424	3812	0.52	1.44	3.61	3.33
	MeCN	340	413	5199	0.49	1.69	2.90	3.02
	DMF	364	442	4848	0.16	1.62	0.99	5.19
	MeOH	368	427	4803	0.56	1.70	3.29	2.59
2D2P	Hexane	376	445	4124	0.79	1.36	5.81	1.54
	Toluene	338	445	7114	0.65	2.73	2.38	1.28
	DCM	333	465	8525	0.94	4.85	1.94	0.12
	THF	336	459	7975	0.86	4.08	2.11	0.34
	MeCN	380	426	2842	0.49	1.03	4.76	4.95
	DMF	334	491	9574	0.42	7.51	0.56	7.72
	MeOH	348	445	6264	0.59	1.97	2.99	2.08

[a] Absorption and emission maxima. [b] Stokes-shift value. [c] Fluorescence quantum yield. [d] Fluorescence lifetime detected at the maximum fluorescence wavelengths. [e] Radiative and nonradiative constants calculated from fluorescence quantum yields and lifetimes.

Table S2 Stokes shifts vs orientation polarizability of **2C2P** and **2D2P** in solvents.

	solvents	f (ε,n) [a]	ν_a (nm) [b]	ν_f (nm) [b]	ν_a-ν_f (cm^{-1}) [c]
2C2P	toluene	0.0123	366	435	4330
	triethylamime	0.0480	364	432	4320
	butyl ether	0.0962	365	432	4250
	ethyl ether	0.1670	330	438	4570
	ethyl acetate	0.1996	364	438	4640
	tetrahydrofuran	0.2095	364	441	4800
	dimethyl formamide	0.2760	362	457	5740
	acetone	0.2843	363	447	5180
2D2P	toluene	0.0123	335	460	8110
	triethylamime	0.0480	334	451	7770
	butyl ether	0.0962	333	455	8050
	ethyl ether	0.1670	330	472	7810
	ethyl acetate	0.1996	331	472	9030
	tetrahydrofuran	0.2095	335	477	8890
	dimethyl formamide	0.2760	334	503	10060
	acetone	0.2843	332	489	9670

[a] The orientation polarizability of solvents; [b] Absorption and emission maxima; [c] Stokes shifts.

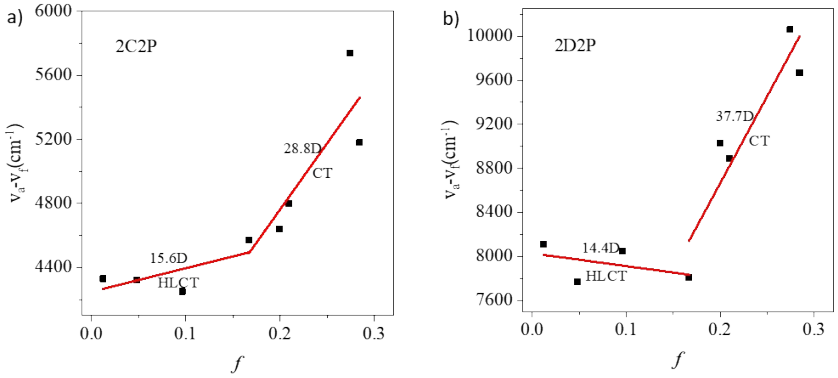

Fig. S2 Lippert-Mataga plots of the enantiomers by Stokes' shifts versus solvent polarizability.

Table S3 Photoluminescence properties of the dyes in PMMA film and in powder.

E_m/Φ_F	Film			Powder
	10% in PMMA	50% in PMMA	Neat	
2C2P	425/0.54	429/0.57	427/0.59	436/0.67
2D2P	443/0.31	443/0.53	448/0.55	448/0.79

PMMA = poly (methylmethacrylate)

Table S4 Calculated excited wavelength (λ), oscillator strengths (*f*) and the related wave functions calculated by using the B3LYP functional with 6-31G(d,p) basis sets.

	State[a]	Energy[b] (eV)	λ[c] (nm)	f[d]	Wave function[e]
2C2P	S_1	3.27	380	0.1141	H→L (95%)
	S_2	3.38	368	0.2799	H-1→L (92%)
	S_3	3.43	362	0.1605	H-3→L (10%), H-2→L (83%)
	S_4	3.54	351	0.0586	H-3→L (86%), H-2→L (10%)
	S_5	3.76	330	0.3942	H→L+1 (27%), H→L+2 (47%)
	S_6	3.76	330	0.1945	H→L+1 (47%), H→L+2 (23%)
	S_7	3.82	325	0.0558	H-2→L+4 (16%), H→L (26%)
	S_8	3.83	324	0.0223	H→L+4 (30%)
	S_9	3.87	321	0.1924	H-2→L+1 (21%), H-1→L+2 (32%)
2D2P	S_1	3.07	404	0.2608	H→L (97%)
	S_2	3.24	383	0.0533	H-1→L (95%)
	S_3	3.40	365	0.1571	H-2→L (94%)
	S_5	3.56	349	0.0426	H-3→L (84%)
	S_6	3.60	345	0.7426	H→L+2 (96%)
	S_7	3.68	338	0.0277	H-1→L+1 (96%)
	S_{10}	3.80	327	0.0331	H-2→L+1 (18%), H-1→L+2 (50%)

[a] Excited state. [b] Calculated energy gaps. [c] Experimental absorption wavelengths [d] Oscillator strength (values < 0.02 are not included). [e] MOs involved in the transitions, H = HOMO, L = LUMO.

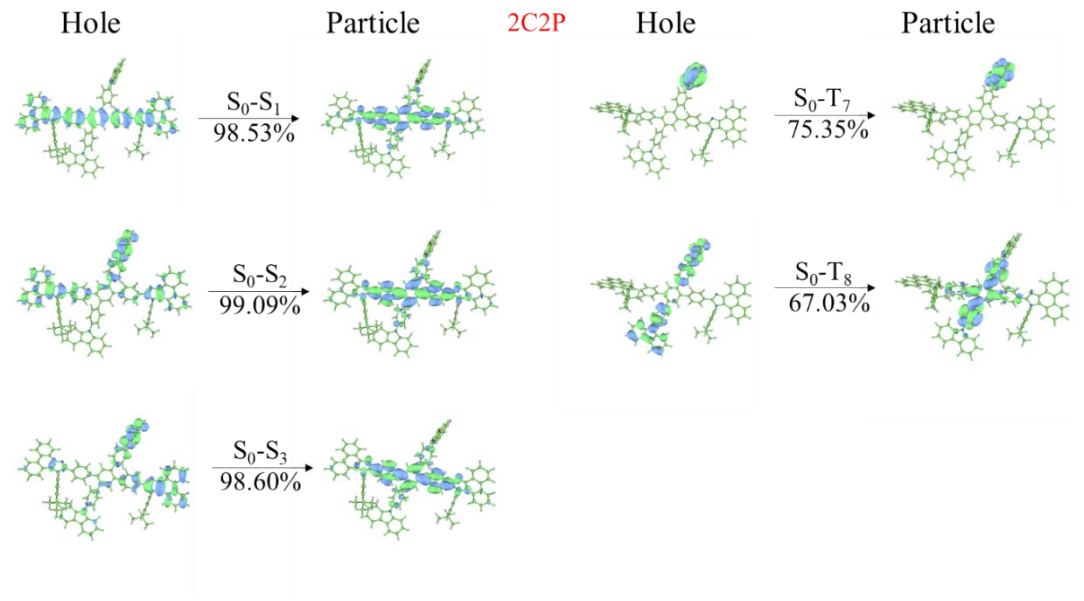

Fig. S3 Natural transition orbitals of S_0 to $S_{1/2/3}$ and S_0 to $T_{7/8}$ for **2C2P**.

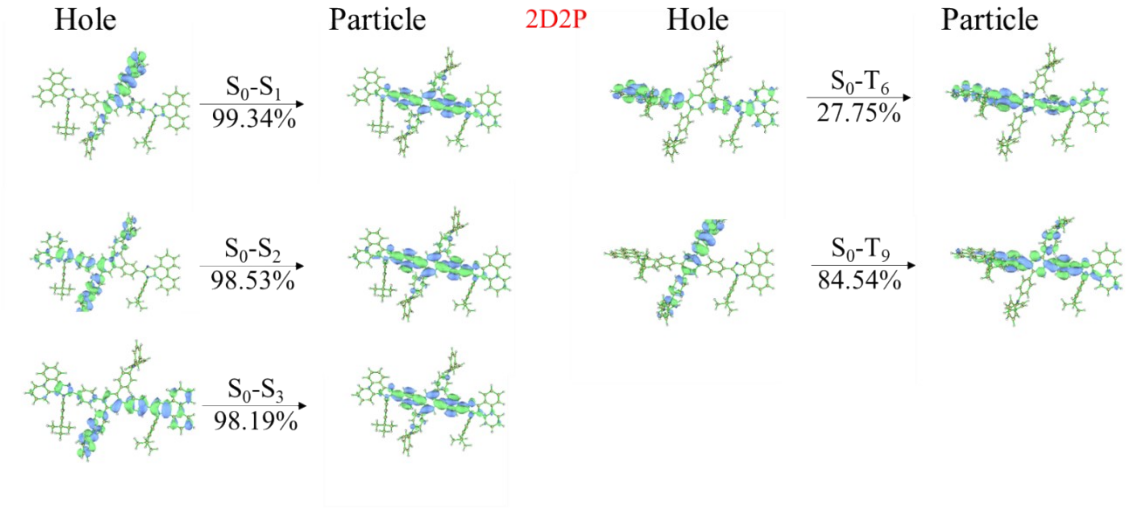

Fig. S4 Natural transition orbitals of S_0 to $S_{1/2/3}$ and S_0 to $T_{6/9}$ for **2D2P**.

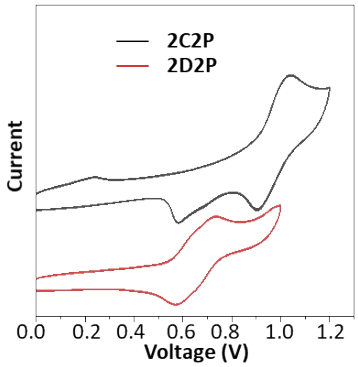

Fig. S5 Cyclic voltammograms curves of **2C2P** and **2D2P**.

Table S5 CV and DFT calculations parameters of compounds

Compounds	E_{ox}[a] (V)	HOMO[b, c] (eV)	LUMO [b, c] (eV)	E_g^{opt} [d] (ev)	E_g^{cal} [e] (ev)
2C2P	0.89	−5.59/−5.18	−2.52/−1.53	3.07	3.65
2D2P	0.53	−5.23/−4.91	−2.19/−1.35	3.04	3.46

[a] Oxidation and reduction potentials from cyclic voltammetry. Ag/Ag+ was used as reference. [b] HOMO was measured from the onset of oxidation curve. LUMO was calculated from HOMO and E_g. [c] Obtained from DFT calculations using b3lyp/6-31g(d,p). [d] Obtained from the cutoff of UV-Vis absorption spectra in DCM. [e] Calculated from the HOMO and LUMO.

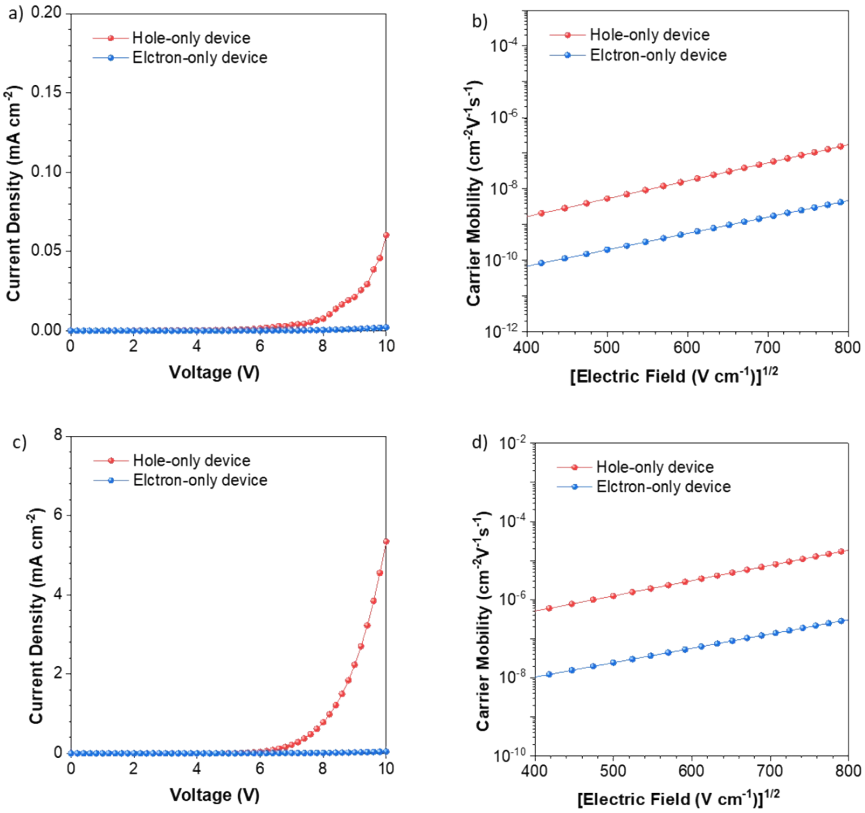

Fig. S6 a, c) J−V curves of the electron-only device (EOD) and hole-only device (HOD) for **2C2P** and **2D2P**, respectively. b, d) Carrier mobility−electric field curves of **2C2P** and **2D2P**, respectively.

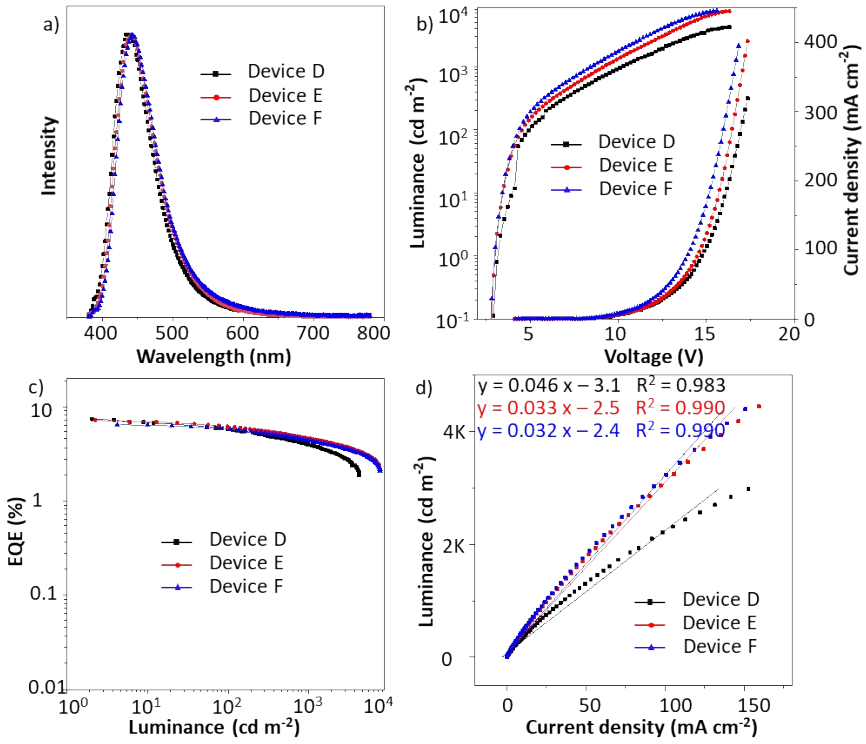

Fig. S7 a) EL spectra of OLEDs for device D−F. b) Luminance and current density vs voltage. c) EQE vs luminance. d) Luminance vs current density (symbol) and the fitted curve plot (line) for device D−F.

II. General details and measurements specifications

Photophysical, thermal and electrochemical property measurements

^{1}H and ^{13}C NMR spectra were recorded on a Bruker AM 400/500 spectrometer. Mass spectrometric measurements were recorded using a MicroQII mass spectrometer. The differential scanning calorimetry (DSC) analysis was performed with 10 ^{o}C min^{-1} heating rate under nitrogen flushing using a TA Instruments DSC 2920. Thermogravimetric analysis was undertaken using a TGA instrument (PE-TGA6) with 20 ^{o}C min^{-1} heating rate under nitrogen. UV-Vis spectra were recorded using a Shimadzu UV-1800 spectrophotometer. Samples for absorption and emission measurements were contained in 1×1 cm quartz cuvettes. Dilute solution with an absorbance of less than 0.05 at the excited wavelength was used for the measurement of fluorescent quantum yields, and the absolutely quantum yields of the materials were determined with a Hamamatsu C13534 spectrometer. Cyclic voltammetric (CV) measurements were carried out in a conventional three-electrode cell, using a Pt button working electrode, a platinum wire counter electrode, and an $Ag/AgNO_3$ reference electrode using a computer-controlled CHI650E at room temperature in dichloromethane (for oxidation) or dimethylformamide (for reduction) containing Bu_4NPF_6 (0.1 M) as the supporting electrolyte.

Device fabrication and EL performance measurements

Glass substrates pre-coated with a 90 nm-thin layer of indium tin oxide (ITO) with a sheet resistance of 15−20 Ω per square were thoroughly cleaned for 10 minutes in ultrasonic bath of acetone, isopropyl alcohol, detergent, deionized water, and isopropyl alcohol and then treated with O_2 plasma for 10 min in sequence. All of the organic materials used were purified by a vacuum sublimation approach. Organic layers were deposited onto the ITO-coated substrates by high-vacuum (< 5×10^{-4} Pa) thermal evaporation. Deposition rates were controlled by independent quartz crystal oscillators, which are 1~2 Å s^{-1} for organic materials, 0.1 Å s^{-1} for LiF, and 5 Å s^{-1} for Al, respectively. The emission area of the devices is 3 mm × 3 mm as shaped by the overlapping area of the anode and cathode. All the device characterization steps were carried out at room temperature under ambient laboratory conditions without encapsulation. EL spectra were taken by normal direction utilizing a spectrometer (Ocean Optics USB 2000+). Luminance−voltages− current density characteristics were measured by PIN-25D silicon photodiode, along with a Keithley 2400 Source Meter. The external quantum efficiencies were estimated utilizing the normalized EL spectra and the current efficiencies of the devices, assuming that the devices are Lambertian emitters.

Carrier mobility calculation

The SCLC property can be described via the *Mott-Gurney* equation (1), and the carrier mobility (μ) of the organic semiconductor can be calculated according to the following Equation (2) (*Poole–Frenkel* formula), where the ε_0 is the vacuum permittivity (8.85×10^{-14} C V^{-1} cm^{-1}), ε_r is the relative dielectric constant (supposed to be 3.0 for organic semiconductor), E stands for the strength of electric field, L is the thickness of emitter, μ_0 is the zero-field mobility, and γ is the *Poole-Frenkel* factor. By fitting the current density–voltage (J–V) curves in SCLC region to Equation (2), the μ_0 and γ values are obtained, thus generating the field-dependent electron mobility according to Equation (2).

$$J = \frac{9}{8}\varepsilon_0\varepsilon_r\mu\frac{E^2}{L} = \frac{9}{8}\varepsilon_0\varepsilon_r\frac{V^2}{L^3}\mu_0 exp\left(0.891\gamma\sqrt{\frac{V}{L}}\right) \quad (1)$$

$$\mu = \mu_0 exp(\gamma\sqrt{E}) \quad (2)$$

Horizontal dipole ratio measurement

For the measurement of the orientation of emitting dipole in molecule, a setup RSQX-01 made by the Changchun Ruoshui Technology Development Co. Ltd. was used. The dipole orientations of doped film were determined by angle-resolved and polarization resolved PL on a half quartz cylinder prism. A continuous-wave He:Cd laser (325 nm) with a fixed angle of 45° to the substrate was employed as excitation source. *p*-Polarized emitted light was detected at the respective peak wavelength of the PL spectrum of each film.

III. ^{1}H NMR spectra of the compounds in CD_2Cl_2

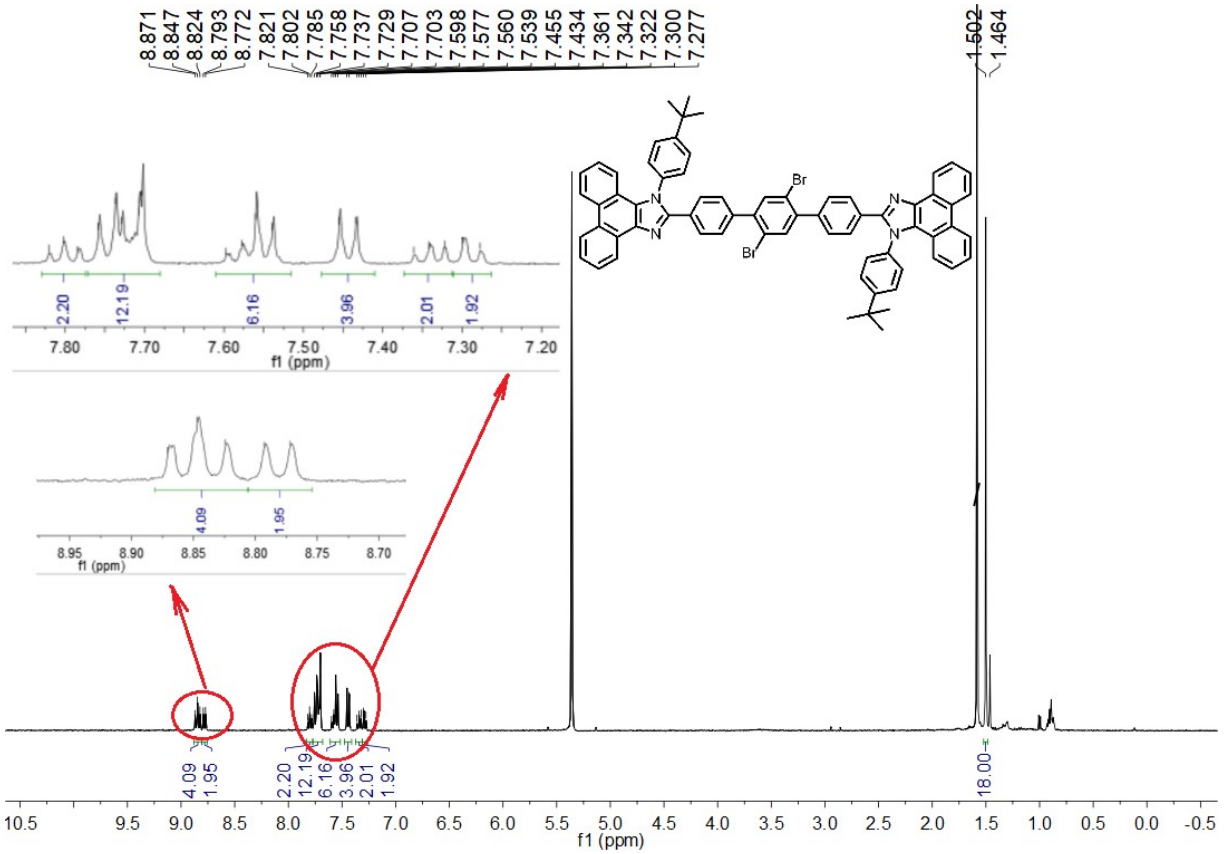

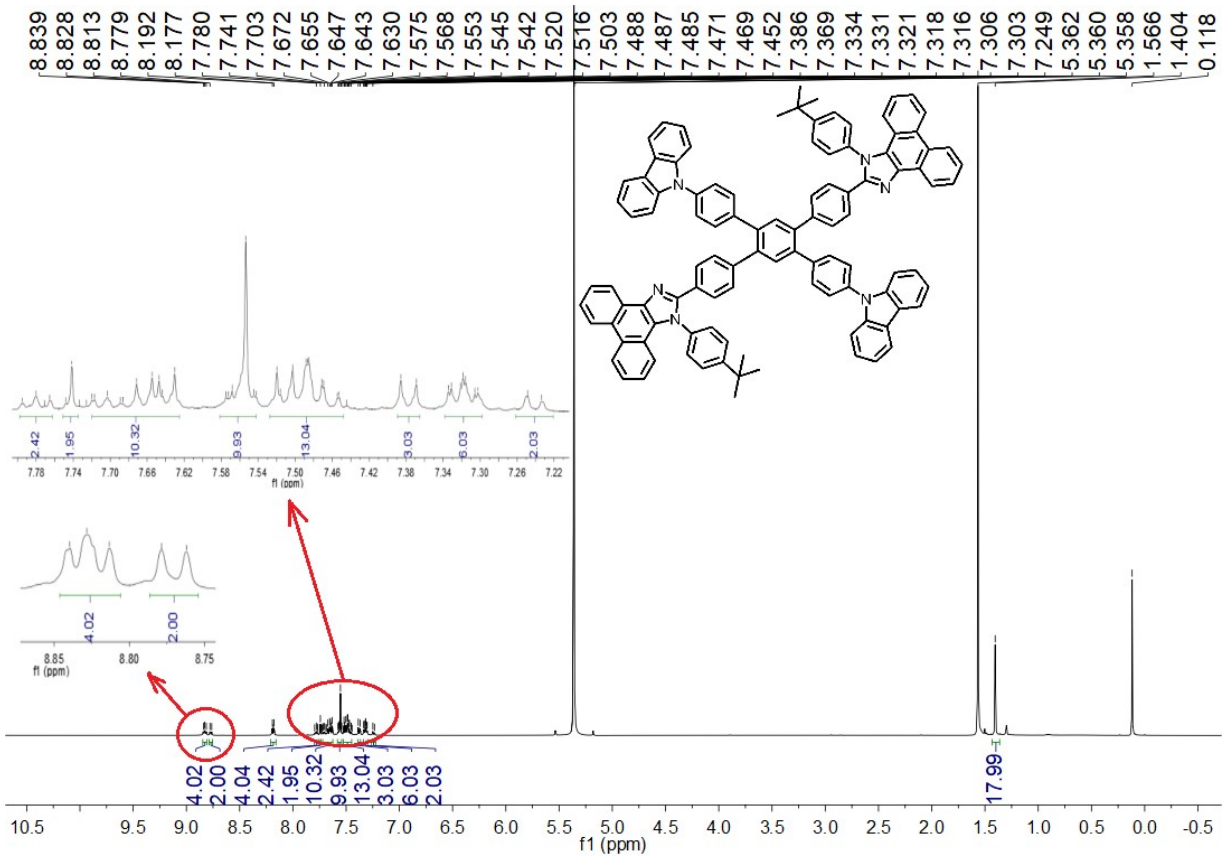

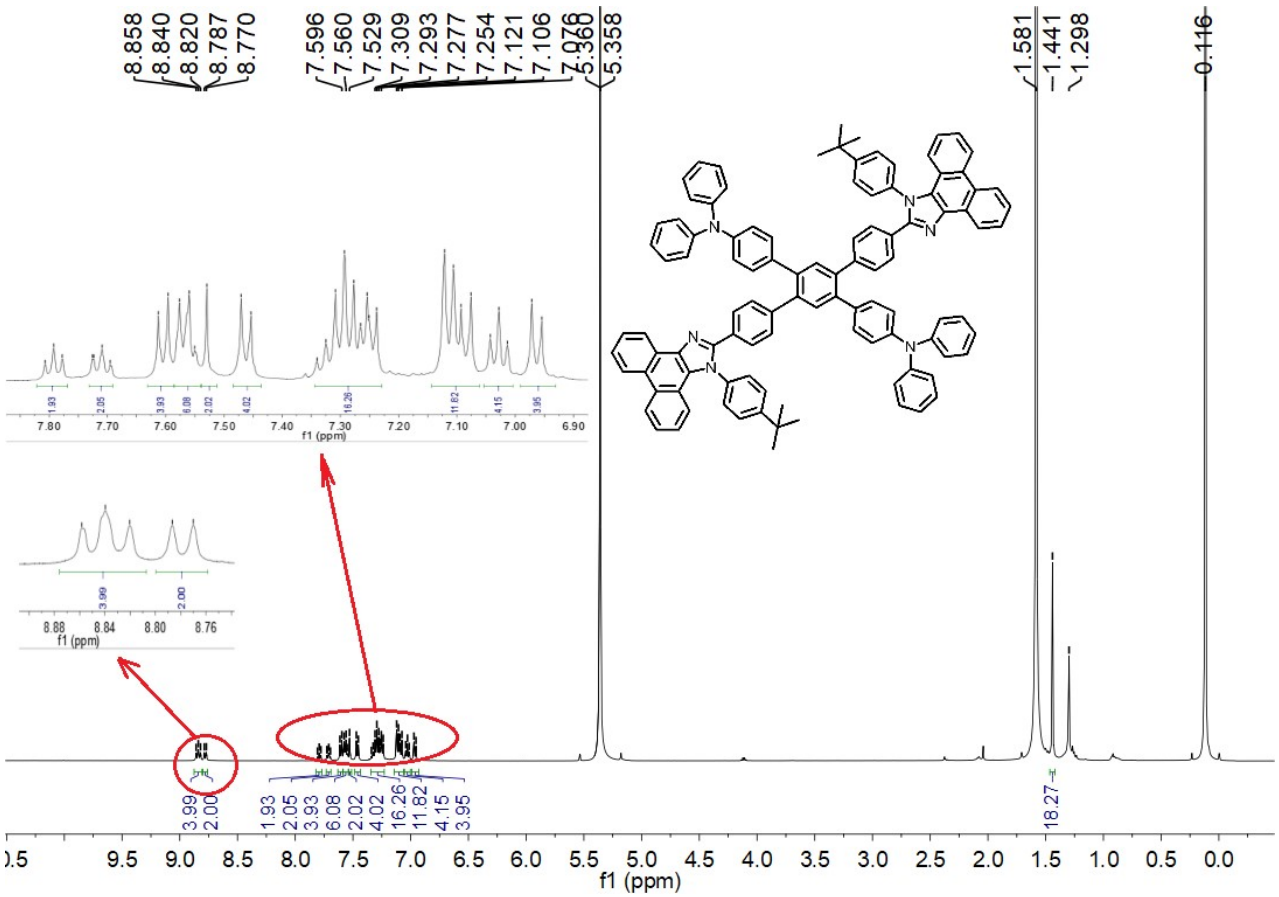
8.858
8.840
8.820
8.787
8.770
7.596
7.560
7.529
7.309
7.293
7.277
7.254
7.121
7.106
7.076
5.368
5.358
1.581
1.441
1.298
0.116
3.99
2.00
1.93
2.05
3.93
6.08
2.02
4.02
16.26
11.82
4.15
3.95
18.27
f1 (ppm)

IV. HR-MS spectra of the target molecules

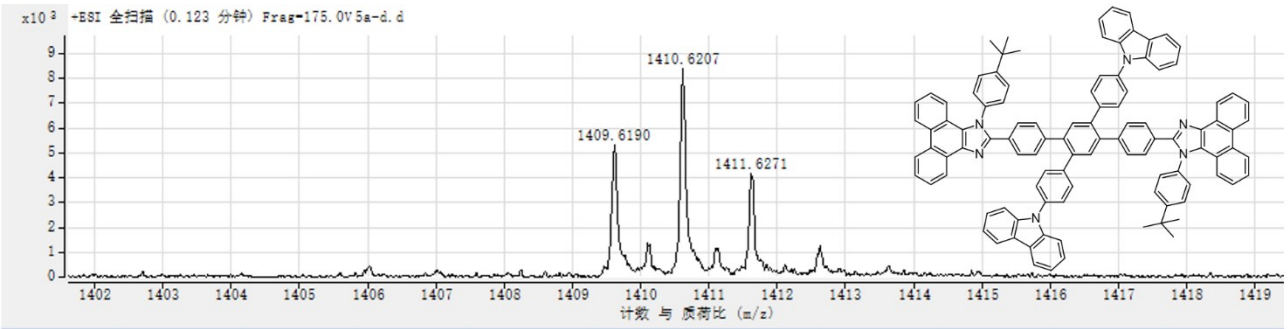

Formula (M)	Ion Formula	Mass	Mass (MFG)	m/z	m/z (Calc)	Diff (ppm)	Diff (mDa)	Abs Diff (ppm)	DBE	Score (MFG)
$C_{104}H_{76}N_6$	$C_{104}H_{77}N_6$	1408.6126	1408.6131	1409.6190	1409.6204	0.99	1.4	0.99	70	100

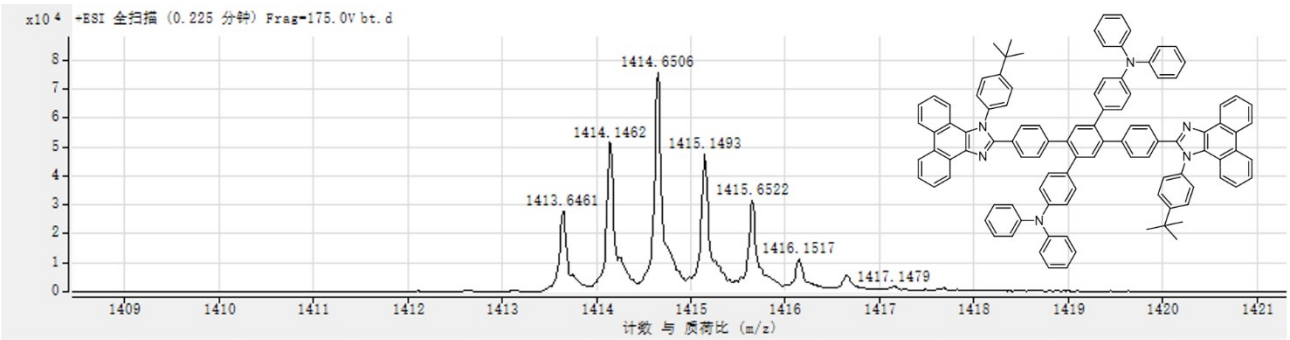

Formula (M)	Ion Formula	Mass	Mass (MFG)	m/z	m/z (Calc)	Diff (ppm)	Diff (mDa)	Abs Diff (ppm)	DBE	Score (MFG)
$C_{104}H_{80}N_6$	$C_{104}H_{81}N_6$	1412.6439	1412.6444	1413.6461	1413.6517	3.9	5.6	3.9	68	100